Engenharia Agrícola
ISSN: 1809-4430 (online)
www.engenhariaagricola.org.br | www.scielo.br/j/eagri

Scientific Paper
DOI: http://dx.doi.org/10.1590/1809-4430-Eng.Agric.v45e20250015/2025

A STUDY ON A MEASUREMENT SYSTEM FOR DETERMINING BULK DENSITY OF UNSATURATED SOILS BASED ON SOIL GAS PERMEABILITY

Shang Gao[1], Xianliang Wang[1*], Yi-Jia Wang[2], Wenqi Zhao[1], Weifan Zhou[1]

[1*]Corresponding author. Institute of Modern Agricultural Equipment, Shandong University of Technology/China, Zibo.
E-mail: wxl1990@sdut.edu.cn | ORCID ID: https://orcid.org/0000-0001-7099-6286

KEYWORDS

Bulk density estimation, soil compaction, soil gas permeability, soil moisture content, soil bulk density.

ABSTRACT

Soil compaction alters soil structure, reduces soil air permeability, and adversely impacts crop growth. However, the rapid field detection of soil compaction remains a significant technical challenge. To address this issue, this study describes the development of an unsaturated soil bulk density measurement system based on soil air permeability, which enables the estimation of soil compaction through the measurement of soil air permeability. The system uses a specially designed soil probe that injects air into the soil at a constant pressure (P_0) and flow rate (Q_0). The steady-state air pressure (ΔP_0) and flow rate (ΔQ_0) at a radius r_0 were recorded to calculate the soil gas permeability coefficient (k_a). Laboratory experiments demonstrated a significant relationship between the soil gas permeability coefficient (k_a), soil bulk density (ρ), and soil moisture content (w): soil compaction, which increases the bulk density, markedly reduces k_a, while a higher soil water content further diminishes air permeability. Using experimental data, a bulk density estimation model was constructed with k_a and w as independent variables. Field validation showed that the model achieved an accuracy of R^2=0.72, thus demonstrating its reliability. This method is operationally straightforward, and allows for the rapid assessment of soil compaction. It provides a robust tool for precision field management and enhanced crop productivity.

INTRODUCTION

The widespread use of large agricultural machinery has caused increasing attention to be paid by soil scientists and farmers to the issue of crop yield reductions caused by soil compaction. Soil compaction is a process in which the soil porosity decreases and bulk density increases under external forces, leading to significant changes in the physical structure and functionality of the soil (Oliveira et al., 2024). Research has demonstrated that excessive compaction markedly increases the packing density of soil particles, thereby reducing soil air permeability and hydraulic conductivity (Liu et al., 2023). These changes hinder gas exchange and restrict the transport and distribution of water and nutrients within the soil. Consequently, these alterations adversely affect crop root respiration and growth, and in severe cases, can result in substantial reductions in crop yield (Fathinejad Poshkoohi et al., 2025; Peralta Ogorek et al., 2024). Consequently, rapid and accurate assessment of soil compaction levels has become a critical focus of soil management and agricultural production research.

Soil bulk density is a widely used indicator for evaluating soil compaction in agriculture, and serves as a fundamental parameter for characterizing soil structure (Suzuki et al., 2022; Yu et al., 2024). From the perspective of soil mechanics, soil compaction is closely associated with changes in pore structure, including alterations in macro-porosity, pore size distribution, and pore connectivity at the microstructural level (Esteban et al., 2024). The contributions of Peters et al. (2025) have provided valuable insights into soil compaction characteristics; however, their methods are limited by the small scale of representation and the

[1] Institute of Modern Agricultural Equipment, Shandong University of Technology/China, Zibo.
[2] Department of Engineering Management, Northeast Agricultural University National Key Laboratory of Smart Farm Technologies and Systems/China, Harbin City.

Area Editor: Fernando António Leal Pacheco
Received in: 1-20-2025
Accepted in: 4-30-2025

complexity of measurement, making them less practical for *in situ* assessments. In recent years, the soil gas permeability coefficient (k_a), an indicator of soil air permeability, has been recognized as an effective parameter for evaluating soil compaction levels (Feng et al.,2023). The soil gas permeability coefficient quantifies the ability of gases to flow through soil, and effectively reflects changes in soil pore structure (Fu et al., 2024; Garg et al., 2021). Research has demonstrated that as soil compaction increases, soil bulk density rises, while pore connectivity and effective pore area decrease significantly, leading to a significant decline in the soil gas permeability coefficient (k_a) (Chen et al., 2021; Chief et al., 2008; Lu et al., 2023; Weeks et al., 1982).

Miao et al. (2010) and Zhan et al. (2016), among others, have noted that soil pores are composed of a combination of the gas and water phases. In dry soils, the gas and solid phases dominate, resulting in relatively large soil pores; in contrast, in moist soils, the proportion of the water phase increases significantly, reducing the gas phase and leading to a substantial decrease in soil pore volume. This dynamic interaction among the water, gas, and solid phases is critical for characterizing the physical properties of soil. Specifically, when estimating soil bulk density, it is essential to account for the effect of soil moisture content (w) on gas flow (Arbor et al., 2024; Mohammadi & Vanclooster, 2019; Wang et al., 2021). Since a single sensor is unable to simultaneously capture the dynamic changes of the solid, liquid, and gas phases within soil, researchers are increasingly exploring the use of multi-sensor integration to enhance measurement accuracy and characterization capabilities. For instance, Hemmat et al. (2014), Naderi-Boldaji et al. (2013) and Quraishi & Mouazen (2013) integrated dielectric sensors with mechanical resistance sensors to develop integrated systems for measuring soil compaction. Similarly, Mouazen et al. (2003) combined soil resistance sensors mounted on agricultural machinery with soil moisture measurement devices, successfully developing a high-precision model for predicting soil bulk density. These studies provide valuable insights and methodological references for advancements in multivariable integrated analysis.

Although both the soil gas permeability coefficient and soil moisture content are critically important parameters for studying soil compaction, there is still a lack of integrated instruments that are capable of simultaneously measuring both. To address this issue, the principles underlying soil air permeability and bulk density variation are combined in this study, and a capacitive moisture sensor is incorporated to create an unsaturated soil bulk density measurement device based on air permeability characteristics. By jointly measuring the soil gas permeability coefficient and moisture content, the proposed device enables the estimation of soil bulk density, thereby facilitating the effective detection of soil compaction.

MATERIAL AND METHODS

Principle of operation

As illustrated in Figure 1, the soil is assumed to behave as a rigid body, with negligible deformation. The soil particles are treated as isotropic and homogeneous, and a continuous gas source within the unsaturated soil is assumed to diffuse spherically and infinitely outward into the surrounding soil. Under these conditions, the gas flow in the soil is in the steady state, and the gas pressure forms spherical isobars. In this state, the soil particles, water, and air are in equilibrium. Equation 1 is employed to estimate the soil gas permeability coefficient (k_a). This equation is theoretically based on the work of Qiu et al. (2021), which describes the steady-state diffusion of airflow in unsaturated soils. A steady-state air pressure (P_0) is applied at the central point, and the pressure diffuses spherically along the boundary and infiltrates the surrounding soil matrix. The corresponding steady-state air pressure variation (ΔP_0) is measured, and when combined with the relationship between the volumetric flow rate (Q_{out}) and the pressure variation (ΔP_0), the soil gas permeability coefficient (k_a) can be accurately determined (Camarda et al., 2006; Li et al., 2021).

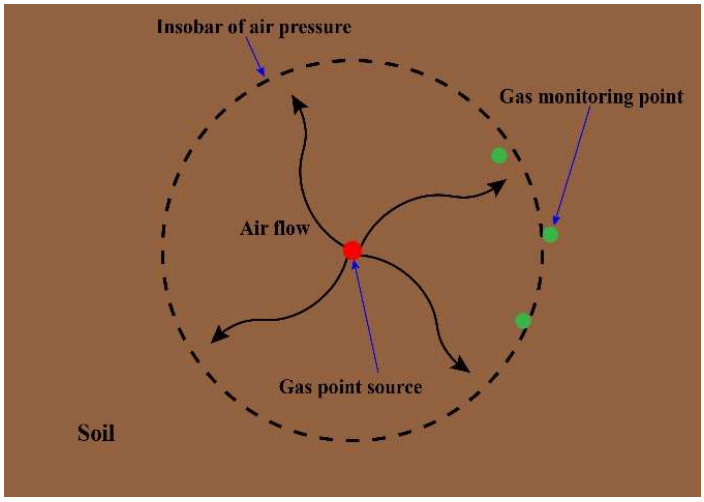

FIGURE 1. Principle of spherical air flow in unsaturated soil.

$$k_a = \frac{Q_{out}\rho_a g}{4r_0\pi\Delta P_0} \quad (1)$$

where: k_a represents the field soil gas permeability coefficient (cm/s), Q_{out} is the measured steady-state gas flow rate (ml/min) required to maintain a constant inflow pressure, and r_0 is the spherical diffusion radius (cm). ρ_a denotes the air density, g is the gravitational acceleration (9.8 m/s^2), and ΔP_0 is the pressure difference across the soil. Once the gas flow through the soil has stabilized, the steady-state flow rate Q_{out} and the pressure difference ΔP_0 are measured, and these values are substituted into [eq. (1)] to compute the soil gas permeability coefficient (k_a).

To estimate soil bulk density, it is essential to account for the combined effects of the soil gas permeability coefficient (k_a) and soil moisture content (w). To ensure the accuracy of the measurement system, the capacitive method is employed in this study to determine soil moisture content. This method is based on the principle that the dielectric constant of water (with a value of approximately 80) is significantly higher than for air (approximately one) and soil particles (approximately three to five). As the soil water content increases, the overall dielectric constant of the soil also increases, enabling precise quantification of changes in soil moisture content.

Device structure and sensors

The structure of the unsaturated soil bulk density measurement system based on soil air permeability is illustrated in Figure 2. The system consists of two functional modules: a soil gas permeability coefficient measurement module, and a soil moisture content measurement module. The measurement probe serves as the core component of the soil bulk density measurement system. This probe consists of a hollow cylindrical tube made of PVC, with an inner diameter of 32 mm, a wall thickness of 3 mm, and a total length of approximately 500 mm. A penetration cone is attached to the probe's tip to facilitate efficient insertion into the soil. Structurally, the probe is divided into three sections: a penetration cone, a perforated section, and a sealed section. The perforated section, which is located directly behind the penetration cone, is 20 mm in length and features uniformly distributed perforations with a diameter of 5 mm. This section allows for air circulation, enabling the injection and recovery of air within the soil. Adjacent to the perforated section is a 40 mm sealed section filled with epoxy resin sealant, which prevents gas leakage between segments. The remaining 360 mm comprises the main body of the probe, which is designed to ensure mechanical stability and precise positioning within the soil.

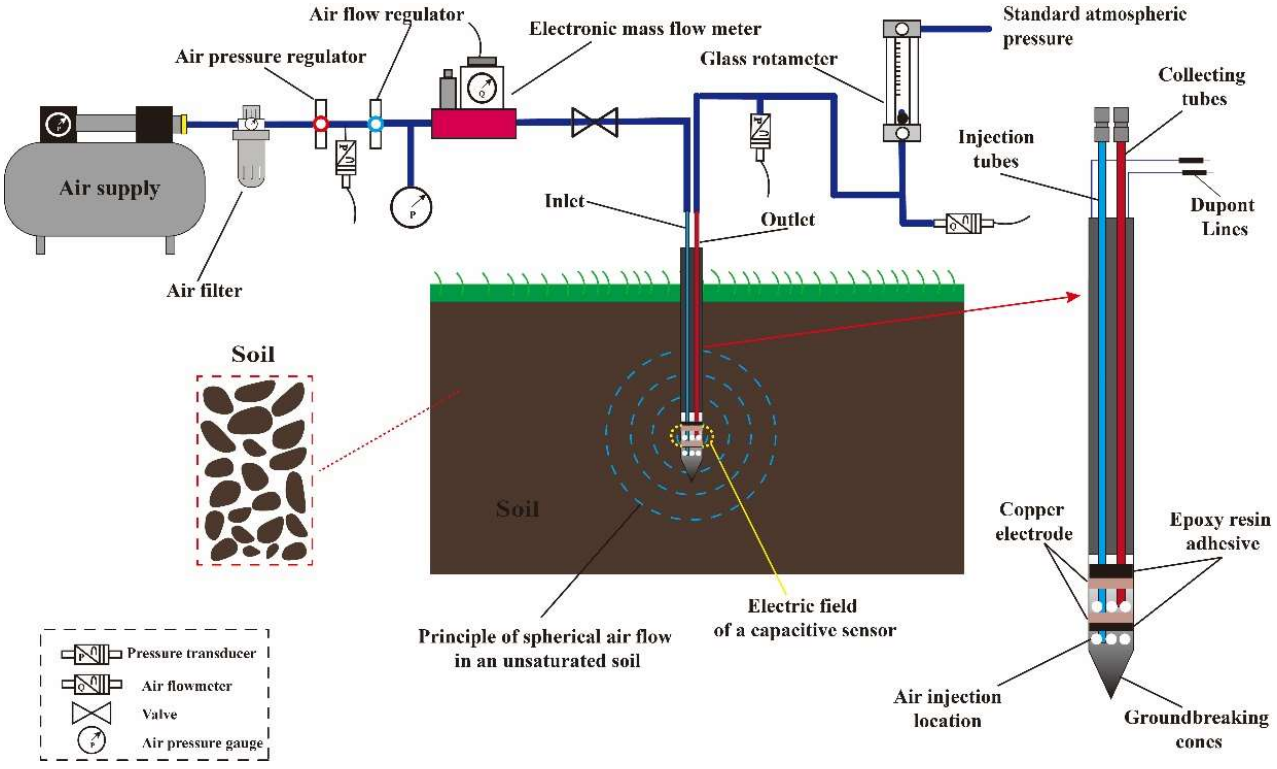

FIGURE 2. Structure of the soil probe and pneumatic circuit.

The internal tubing of the soil probe includes an air injection tube and an air collection tube, which are designed for air injection and collection during measurements. The air injection tube terminates at the lower part of the perforated section, while the air collection tube extends through the sealed section to the upper part of the second perforated section. To prevent soil particles from clogging the air holes, the upper and lower perforated sections are filled with 3–5 mm porous ceramic balls. The system is connected to an external air compressor via the air injection tube. Air pressure and flow rate are regulated using an air pressure regulator and a flow control valve installed along the tubing. A pressure transmitter and an electronic mass flow meter monitor the air pressure and volumetric flow rate. During testing, no

significant gas pressure differences (<0.01 kPa) were observed, meaning that the pressure loss in the tubing was negligible. The soil moisture content measurement module includes an FDC2214 capacitive sensor, which is combined with an external ring electrode attached to the soil probe. The FDC2214 sensor detects variations in capacitance via its internal L-C resonator, and converts these into digital signals corresponding to the effective dielectric constant of the soil. By leveraging the high dielectric constant characteristic of water, the soil moisture content can be estimated.

Calibration of sensors

For the measurement of soil moisture content, the capacitance method was adopted in this study, using a high-sensitivity FDC2214 capacitive sensor. To ensure the accuracy of measurement, calibration was conducted in accordance with the sensor manual. Calibration of the FDC2214 module was performed using standard soil samples with varying moisture contents, following a controlled natural air-drying procedure.

To prepare the standard soil samples, the excavated soil was oven-dried, crushed, and sieved through a 2 mm mesh to remove impurities. Based on the volume of the soil containers, the dry soil was evenly divided into six portions and placed into containers, and the total dry soil mass was recorded. The weighed soil samples were then soaked in water for 24 h to achieve full saturation, and subsequently allowed to equilibrate for 2 h. At this stage, the FDC2214 moisture detection module was inserted into the soil samples to record the initial capacitance values and corresponding soil weights. Following this, the samples underwent gradual natural air-drying, with the output values of the FDC2214 sensor and the total soil mass recorded at 8-h intervals.

Measurement and analysis of soil bulk density

For preparation of the standard soil samples, farmland soil was collected from Xilü Village and Xiangyang Village in Zhangdian District, Zibo City, Shandong Province (118.03°N, 36.82°E). To simulate field soil conditions, soil samples with target moisture contents of 8%, 12%, 16%, 20%, and 24% were prepared and packed into aluminum buckets with a diameter of 300 mm and a height of 500 mm. Following sample preparation, the soil samples were layered into the aluminum buckets at the target bulk densities (ρ) of 1.0, 1.15, 1.30, 1.45, and 1.60 g/cm³. Each layer was 5 cm thick, and after filling, each layer was compacted using a standard rammer to ensure that the achieved bulk density met the target value, with an error margin that was controlled to within ±0.05 g/cm³.

Before the experiment, a vertical hole with a diameter of 40 mm and a depth of 350 mm was drilled into the center of the soil column using a drill bit. Care was taken to ensure that the wall of the hole was smooth and that disturbance to the surrounding soil structure was minimized. When the soil probe was securely fixed, petroleum jelly was applied to the surfaces of both the probe and the soil sample to create an airtight seal, thereby preventing gas leakage that could affect the measurement results.

Following this setup process, the pressure and flow control switches were adjusted, with the initial air injection pressure set to 10 kPa and the gas inflow rate controlled at 150 mL/min. This moderate flow rate was chosen to ensure uniform diffusion of the gas within the soil while avoiding potential structural damage or abnormal pressure fluctuations caused by excessive airflow. When the inlet valve was opened, air with a constant volumetric flow rate was injected into the soil at the specified initial pressure. Throughout the injection process, the gas flow rate and pressure were monitored in real time, and measurements of gas pressure and flow rate were recorded at 5-min intervals. When the system reached a quasi-steady state—defined as a change in gas pressure of less than 0.01 kPa and a flow rate fluctuation of less than 1% within 10 min—the steady-state gas flow rate (Q) and the corresponding differential pressure (ΔP_0) were recorded. These data were then substituted into Equation 1 to calculate the soil gas permeability coefficient (k_a). Each measurement was repeated three times to ensure the reliability and stability of the results. When the experiment was complete, data processing and statistical analysis were conducted using SPSS 26.0, and a linear regression analysis was performed to establish a functional relationship between the soil gas permeability coefficient (k_a), soil moisture content (w), and soil bulk density (ρ), which provided insights into the interactions among these variables and their respective effects on soil bulk density.

Experimental results and discussion

Validation of capacitive sensor for soil water content

A capacitive moisture sensor operates by detecting changes in the dielectric properties between its capacitor plates, which reflect variations in capacitance. The measured capacitance value is positively correlated with the dielectric constant of the material between the plates. Throughout the 17-day air-drying process, a strong linear relationship was observed between soil moisture content and the capacitance values measured by the sensor, with a correlation coefficient of R^2= 99.4%, as illustrated in Figure 3.

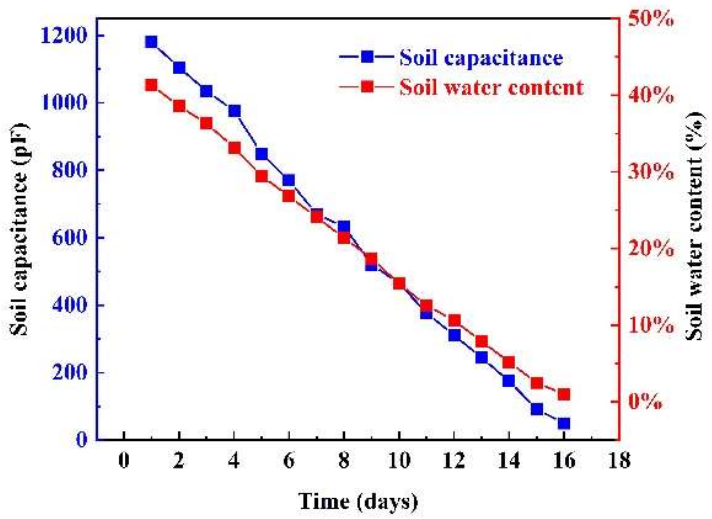

FIGURE 3. Validation of capacitance sensors: relationship between soil capacitance and moisture content.

A comprehensive analysis revealed no significant effect of soil texture on the readings of the capacitive sensor, suggesting that while soil texture or organic matter content may have a minor influence on the dielectric properties of the soil, the effect is not statistically significant. Similarly, Kargas et al. (2013), using a novel dielectric constant sensor to measure the dielectric properties of soils with varying moisture levels, also reported that soil texture did not significantly affect sensor readings. However, their study identified that soil salinity and temperature introduced measurable interference effects on sensor data.

Measurement of soil permeability coefficients

Figure 4(a) depicts the variation in the soil gas permeability coefficient (k_a) with bulk density under different soil moisture contents. At all five moisture levels, the gas permeability coefficient decreases significantly as the bulk density increases, but the magnitude of the decline varies depending on the moisture content. For instance, at a relatively low moisture content (w=12%), the gas permeability coefficient decreases by approximately two orders of magnitude as bulk density increases from 1.0 g/cm³ to 1.6 g/cm³.

Analysis reveals that when the moisture content is below 16%, the slopes of the gas permeability coefficient curves are steeper under different bulk densities. This suggests that at low moisture levels, the pore system of the soil predominantly governs the gas flow. This behavior can be attributed to the presence of abundant gas-phase pores in the soil at lower moisture content and minimal compaction, which facilitates easier gas transport. In contrast, when the soil moisture content exceeds 16%, the rate of decline in the gas permeability coefficient diminishes; this may be because the higher water content increasingly fills the pore space with water, and compaction further reduces the pore connectivity. Under these conditions, the pathways available for gas flow are extremely limited, and further increases in bulk density have a reduced marginal impact on the gas permeability coefficient (Wang et al., 2009). These findings suggest that at higher moisture content, the primary limitation on soil gas permeability changes from the bulk density to the proportion of pore space occupied by water.

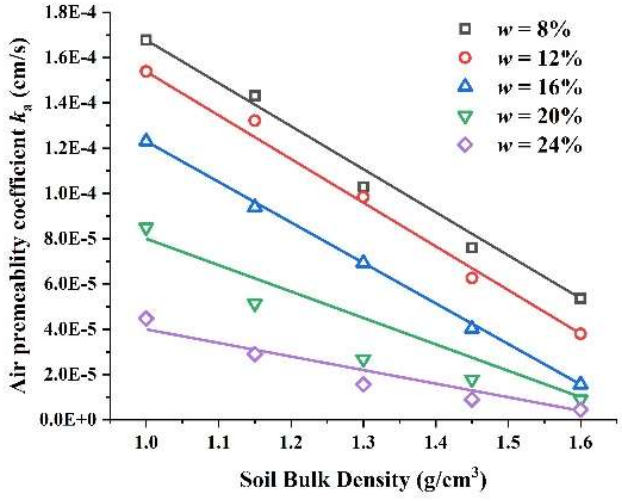

(a) Variation in soil air permeability coefficient with bulk density

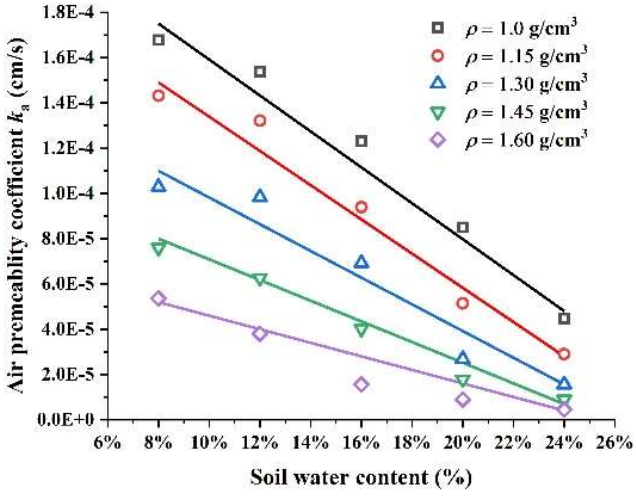

(b) Variation in soil air permeability coefficient with soil water content

FIGURE 4. Correlation between k_a and ρ in two different textured soils.

Figure 4(b) illustrates the variation in the gas permeability coefficient with moisture content under different bulk density conditions. At a fixed bulk density, the gas permeability coefficient decreases significantly with increasing moisture content. For example, at a bulk density of 1.2 g/cm³, increasing the moisture content from 8% to 24% results in a decrease in the gas permeability coefficient of more than one order of magnitude. This indicates that as the soil moisture content rises, water progressively occupies the pore space, thereby obstructing gas flow.

An analysis of the curve shapes also reveals that as bulk density increases, the curves for different moisture contents gradually converge. This implies that at high bulk density, the effects of soil compaction become the dominant constraint on gas flow, surpassing the influence of moisture content. These observations are consistent with the findings of Charlotte et al., who reported that during soil compaction, as bulk density increases, larger pores are progressively compressed into smaller pores, leading to a significant reduction in porosity and pore size (Van Verseveld & Gebert, 2020). This reduction in porosity restricts the diffusion of gases in the soil, forcing the gas flow through increasingly narrow pathways.

Figures 4(a) and (b) demonstrate that the soil gas permeability coefficient (k_a) is jointly influenced by soil bulk density (ρ) and moisture content (w). At a lower moisture content, the soil pore system is predominantly in the gas phase, and the effect of increasing the bulk density on the gas permeability coefficient is particularly significant. In contrast, at higher moisture content, water progressively fills the pore space, further compressing the pathways available for gas flow and resulting in a reduced rate of decline in the gas permeability coefficient.

In addition, as the bulk density increases, the differences in gas permeability coefficients across varying moisture levels gradually diminish, indicating that at a high bulk density, the inhibitory effect of compaction on gas flow surpasses the influence of moisture content. These findings show that soil air permeability is governed by the combined effects of pore structure and moisture content.

Models for estimating soil bulk density

It is noteworthy that the soil bulk density (ρ) can be predicted solely based on the soil gas permeability coefficient (k_a), as a higher soil compaction corresponds to reduced air permeability, and vice versa. However, this strong correlation may rely on the spatial uniformity of soil moisture and particle size distribution across the measurement site. Furthermore, the experimental soil may contain clay and organic matter, which undergo swelling and contraction during water absorption and flow, thereby affecting the gas permeability coefficient (k_a). To develop a physically meaningful prediction model for soil bulk density (ρ), the two primary influencing factors of gas permeability coefficient (k_a) and soil moisture content (w) were used as independent variables.

To allow us to quantify the relationship between soil bulk density, gas permeability, and soil moisture content more effectively, the ratio of the gas permeability coefficient to soil moisture content (k_a/w) was introduced as an independent variable for further functional analysis of the prediction model. As shown in Figure 5, the relationship between gas permeability and moisture content follows a consistent trend under varying bulk density conditions. A standardized residual regression analysis of the experimental data revealed that the residuals exhibit a normal distribution, confirming the validity of the linear relationship between the independent variables (k_a and w) and the dependent variable (ρ).

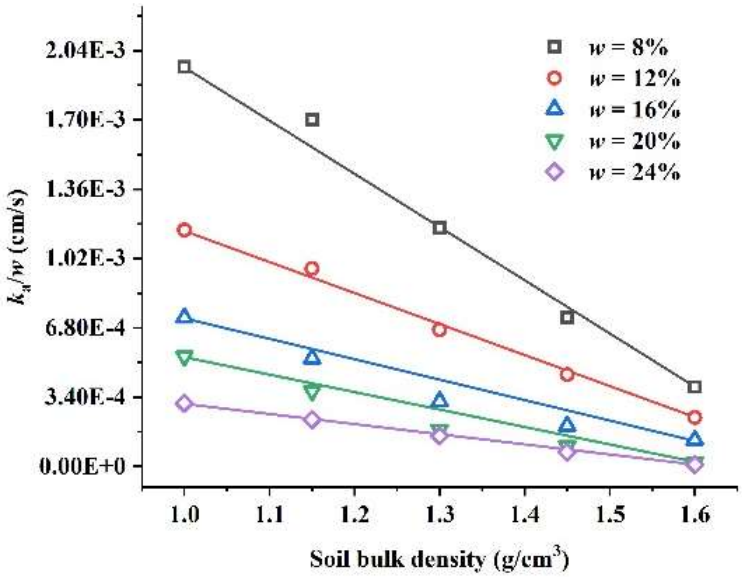

FIGURE 5. Relationship between the ratio of soil gas permeability coefficient to soil water content and the soil bulk density.

A multivariate linear regression effectively captured the relationships among k_a, w, and ρ, and a regression analysis indicated that variations in soil moisture content (w) not only directly influence the gas permeability coefficient (k_a) but also indirectly impact bulk density (ρ) by altering pore connectivity. Using a multivariate linear regression in SPSS, the functional relationship among gas permeability (k_a), soil moisture content (w), and soil bulk density (ρ) was determined, as shown in [eq (2)]. The prediction model gave a coefficient of determination (R^2) of 86.23% with a significance level of $P<0.001$, indicating strong predictive reliability.

$$\rho=2.26-5.91k_a\times10^3-3.53w \quad (2)$$

In Equation 2: k_a represents the soil gas permeability coefficient (cm/s); w denotes the soil moisture content (%); ρ is the soil bulk density (g/cm³); and β_1, β_2, and β_3 are regression coefficients, which depend on the soil texture. In this study, the values of the regression coefficients are determined as follows: $\beta_1=2.26$, $\beta_2=-5.91\times10^3$, and $\beta_3=-3.53$.

Field trials and validation

To validate the accuracy of the proposed bulk density estimation model, a field experiment was conducted in farmland located in Xiangyang Village, Zhangdian District, Zibo City, Shandong Province (118.03°N, 36.82°E). Measurements of undisturbed soil bulk density were performed at various locations to evaluate the model, as illustrated in Figure 6. Before the experiment, a 40 mm soil drill was used to create vertical boreholes at depths of 150, 300, and 450 mm. The soil probe was inserted into the boreholes, and the system was activated to collect the soil gas permeability coefficient (k_a) and soil moisture content (w), which were then substituted into Equation 2 to calculate the estimated soil bulk density (ρ). After completing the probe measurements, soil profiles were excavated using a spade along the side of the boreholes. Soil samples surrounding the probe measurement points were collected using a cutting ring to determine the actual soil bulk density, which was compared with the probe measurement results.

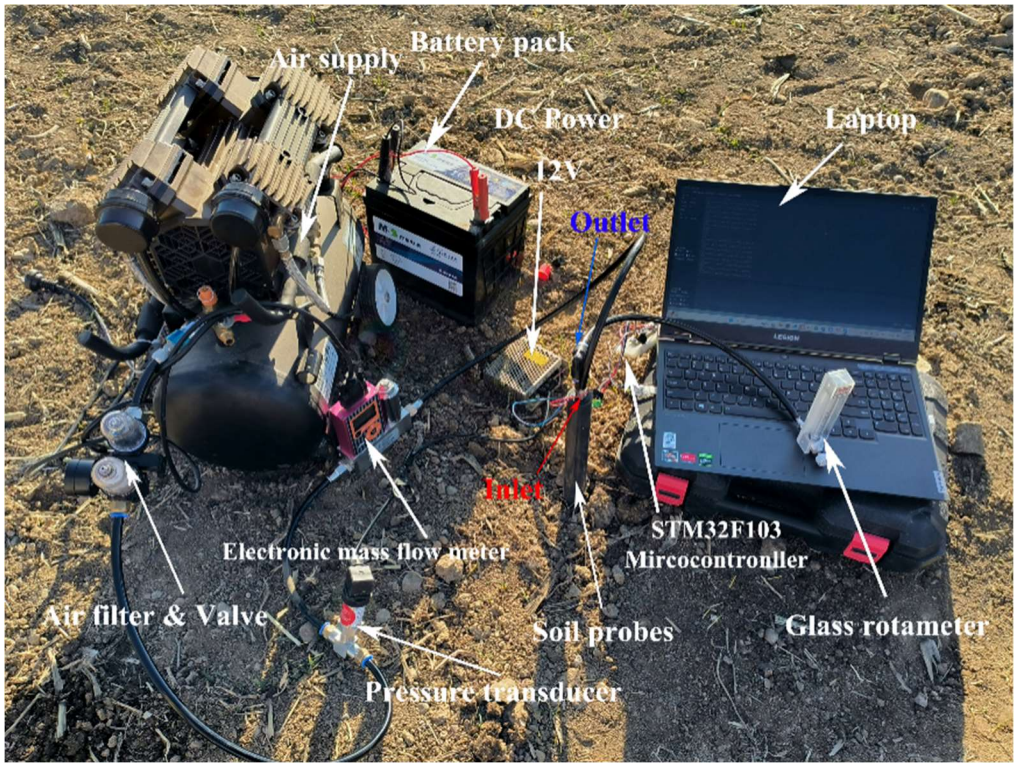

FIGURE 6. Proposed bulk density measurement system employed to measure the bulk density of unsaturated soil under field conditions.

A comparison of the soil compaction results obtained from the ring knife method indicated that the relative error between the two measurement methods fluctuated between −6.12% and 8.13%, with an average relative error of 6.09%, as shown in Figure 7. An absolute error of 8.1% was observed in the experiment. Analysis of the measurement environment suggests that this discrepancy may be due to the high stone content in the lower soil layers, which disrupted the uniformity of the soil. The presence of partially decomposed straw also affected the contact between the soil probe and the soil, thereby impacting the measurement accuracy.

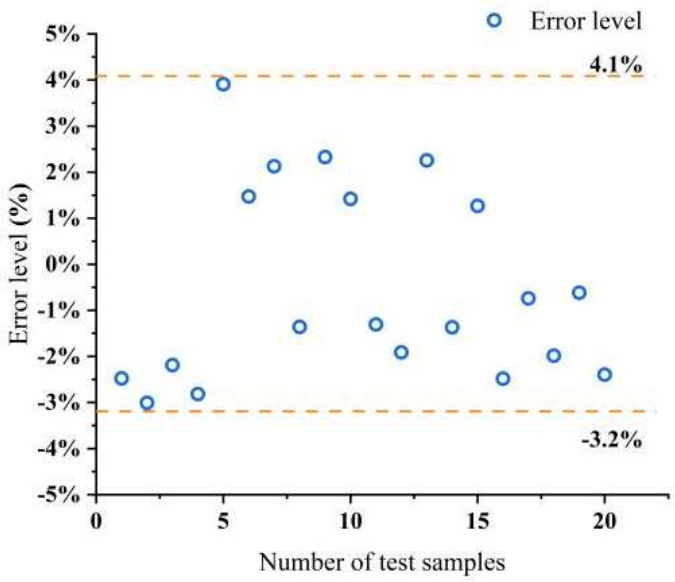

FIGURE 7. Relative error between two soil bulk density testing methods.

Figure 8 illustrates the validation and evaluation of the model using experimental data. The results indicate that the model exhibits a high degree of fit in estimating the variation trends of soil bulk density (ρ) and effectively predicts ρ under various conditions.

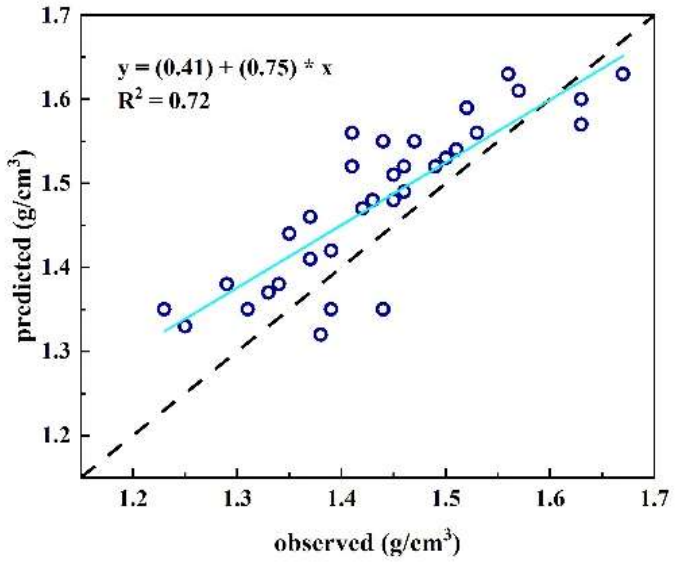

FIGURE 8. Correlation between predicted ρ values and *in situ* observations.

In summary, we find that the soil bulk density estimation system effectively estimates bulk density across different regions while simultaneously measuring soil moisture content. The results confirm that soil air permeability can serve as a reliable metric for characterizing soil compaction. By introducing the soil gas permeability coefficient (k_a), a predictive model for bulk density could be developed that included key factors. This model supports the continuous monitoring of field compaction based on air permeability and moisture content, and can offer valuable insights in terms of optimizing agricultural management, improving soil conditions, and boosting crop yields. These findings promote sustainable agricultural practices and highlight the importance of precise soil monitoring systems.

CONCLUSIONS

Based on the relationship between soil air permeability and bulk density, as well as the theory of spherical gas diffusion within soil, a novel soil bulk density estimation system was developed. This system combined the principles of unsaturated soil spherical gas flow with a capacitive moisture sensor, resulting in a new sensor that is capable of simultaneously measuring soil gas permeability coefficient (k_a) and soil moisture content (w). By analyzing variations in soil air permeability (k_a), the system estimates soil bulk density (ρ) and accurately detects soil compaction states. Field experiments produced the following key findings:

(1) Within the soil texture range of the Huang-Huai-Hai region in China, evaluations of the capacitive sensor indicated that soil texture does not significantly affect the

measurement accuracy. Furthermore, the impact of organic matter content on the sensor's capacitance readings was minimal. The capacitive sensor demonstrated strong adaptability and reliability across various soil textures, although the influence of variations in organic matter content on the measurement accuracy should still be considered.

(2) The soil probe showed significant potential for measuring soil air permeability and estimating soil bulk density. Its working principle is based on detecting changes in gas diffusion characteristics within the soil to characterize bulk density. By leveraging the strong correlation between soil air permeability and bulk density, the soil probe effectively captures variations in soil compaction. When combined with soil moisture content measurements, the probe provides a practical and efficient method for estimating bulk density and rapidly detecting compaction states across different soil types.

(3) A three-parameter estimation model for soil bulk density (ρ) was successfully developed and evaluated. The model integrated the soil gas permeability coefficient (k_a) and soil moisture content (w) as independent variables, and provided a reliable tool for bulk density estimation.

In summary, this system provides a robust framework for the intensity of monitoring soil compaction and bulk density under varying soil conditions. By introducing soil gas permeability as a key parameter for representing changes in soil structure, the study lays the foundation for continuous monitoring of soil compaction intensity in agricultural fields. In addition, the system offers valuable scientific support for optimizing agricultural management practices, improving soil conditions, and enhancing crop productivity.

ACKNOWLEDGMENTS

This work was supported financially by the National Natural Science Foundation of China (Grant No. 32101631), and the Shandong Integrated Agricultural Machinery R&D, Production, Promotion & Application Pilot (NJYTHSD-202315).

REFERENCES

Arbor, A., Schmidt, M., Zhang, J., Bulmer, C., Filatow, D., Kasraei, B., & Heung, B. (2024). Filling the gaps in soil data: A multi-model framework for addressing data gaps using pedotransfer functions and machine-learning with uncertainty estimates to estimate bulk density. *CATENA*, *245*, 108310. https://doi.org/https://doi.org/10.1016/j.catena.2024.108310

Camarda, M., Gurrieri, S., & Valenza, M. (2006). In situ permeability measurements based on a radial gas advectionModel: relationships between soil permeability and diffuse CO2 degassing in volcanic areas. *Pure and Applied Geophysics*, *163*(4), 897-914. https://doi.org/10.1007/s00024-006-0045-y

Chen, R., Huang, J.-W., Zhou, C., Ping, Y., & Chen, Z.-K. (2021). A new simple and low-cost air permeameter for unsaturated soils. *Soil and Tillage Research*, *213*, 105083. https://doi.org/https://doi.org/10.1016/j.still.2021.105083

Chief, K., Ferré, T. P. A., & Nijssen, B. (2008). Correlation between air permeability and saturated hydraulic conductivity: unburned and burned soils. *Soil Science Society of America Journal*, *72*, 1501-1509.

Esteban, D. A. A., Souza, Z. M. de, Tormena, C. A., Gomes, M. G. dos S., Parra, J. A. S., Guimarães Júnnyor, W. da S., & Moraes, M. T. de. (2024). Risk assessment of soil compaction due to machinery traffic used in infield transportation of sugarcane during mechanized harvesting. *Soil and Tillage Research*, *244*, 106206. https://doi.org/https://doi.org/10.1016/j.still.2024.106206

Fathinejad Poshkoohi, A., Mohammadi, M. H., Zarebanadkouki, M., & Etesami, H. (2025). Mucilage increases soil resistance to penetration after compaction. *Rhizosphere*, *33*, 101014. https://doi.org/https://doi.org/10.1016/j.rhisph.2024.101014

Feng, S., Sun, J. X., Zhan, L. T., & Liu, H. W. (2023). A new method and instrument for measuring in situ gas diffusion coefficient and gas coefficient of permeability of unsaturated soil. *Journal of Geotechnical and Geoenvironmental Engineering*, *149*(7).

Fu, Z., Yan, Z., & Li, S.-l. (2024). Effects of soil pore structure on gas diffusivity under different land uses: Characterization and modelling. *Soil and Tillage Research*, *237*, 105988. https://doi.org/https://doi.org/10.1016/j.still.2023.105988

Garg, A., Huang, H., Cai, W., Reddy, N. G., Chen, P., Han, Y., & Zhu, H.-H. (2021). Influence of soil density on gas permeability and water retention in soils amended with in-house produced biochar. *Journal of Rock Mechanics and Geotechnical Engineering*, *13*(3), 593-602. https://doi.org/https://doi.org/10.1016/j.jrmge.2020.10.007

Hemmat, A., Rahnama, T., & Vahabi, Z. (2014). A horizontal multiple-tip penetrometer for on-the-go soil mechanical resistance and acoustic failure mode detection. *Soil and Tillage Research*, *138*, 17-25. https://doi.org/https://doi.org/10.1016/j.still.2013.12.003

Kargas, G., Ntoulas, N., & Nektarios, P. A. (2013). Soil texture and salinity effects on calibration of TDR300 dielectric moisture sensor. *Soil Research*, *51*, 330-340.

Li, X.-A., Wang, L., Xue, Q., Zheng, H., Hong, B., Li, L.-C., & Lei, H.-n. (2021). In situ field measurements of air permeability in eroded loess formations. *Environmental Earth Sciences*, *80*(4), 137. https://doi.org/10.1007/s12665-021-09377-0

Liu, B., Jing, Z., Wang, J., & Feng, Y. (2023). Effect of soil compaction on hydraulic properties and macropore structure: Evidence from opencast mines in the Loess Plateau of China. *Ecological Engineering*, *192*, 106988. https://doi.org/https://doi.org/10.1016/j.ecoleng.2023.106988

Lu, S.-F., Han, Z.-J., Xu, L., Lan, T.-G., Wei, X., & Zhao, T.-Y. (2023). On measuring methods and influencing factors of air permeability of soils: An overview and a preliminary database. *Geoderma*, *435*, 116509. https://doi.org/https://doi.org/10.1016/j.geoderma.2023.116509

Miao, Q.-q., Chen, Z.-h., Zhang, L., Huang, X.-f., & Qian, N.-g. (2010). Experimental study of gas permeability of unsaturated clayey sand. *Rock and Soil Mechanics*, *31*(12), 3746 - 3750. http://ytlx.whrsm.ac.cn/CN/abstract/article_9270.shtml

Mohammadi, M. H., & Vanclooster, M. (2019). A simple device for field and laboratory measurements of soil air permeability. *Soil Science Society of America Journal*. https://doi.org/10.2136/sssaj2018.03.0114

Mouazen, A. M., Dumont, K., Maertens, K., & Ramon, H. (2003). Two-dimensional prediction of spatial variation in topsoil compaction of a sandy loam field-based on measured horizontal force of compaction sensor, cutting depth and moisture content. *Soil and Tillage Research*, *74*(1), 91-102. https://doi.org/https://doi.org/10.1016/S0167-1987(03)00123-5

Naderi-Boldaji, M., Sharifi, A., Alimardani, R., Hemmat, A., Keyhani, A., Loonstra, E. H., & Keller, T. (2013). Use of a triple-sensor fusion system for on-the-go measurement of soil compaction. *Soil and Tillage Research*, *128*, 44 - 53. https://doi.org/https://doi.org/10.1016/j.still.2012.10.002

Oliveira, E. M., Wittwer, R., Hartmann, M., Keller, T., Buchmann, N., & van der Heijden, M. G. A. (2024). Effects of conventional, organic and conservation agriculture on soil physical properties, root growth and microbial habitats in a long-term field experiment. *Geoderma*, *447*, 116927. https://doi.org/https://doi.org/10.1016/j.geoderma.2024.116927

Peralta Ogorek, L. L., Gao, Y., Farrar, E., & Pandey, B. K. (2024). Soil compaction sensing mechanisms and root responses. *Trends in Plant Science*. https://doi.org/https://doi.org/10.1016/j.tplants.2024.10.014

Peters, A., Germer, K., Naseri, M., Rolfes, L., & Lorenz, M. (2025). Modeling compaction effects on hydraulic properties of soils using limited information. *Soil and Tillage Research*, *246*, 106349. https://doi.org/https://doi.org/10.1016/j.still.2024.106349

Qiu, Q. W., Zhan, L. T., Leung, A. K., Feng, S., & Chen, Y. M. (2021). A new method and apparatus for measuring in situ air permeability of unsaturated soil. *Canadian Geotechnical Journal*, *58*(4), 514-530. https://doi.org/10.1139/cgj-2019-0733

Quraishi, M. Z., & Mouazen, A. M. (2013). A prototype sensor for the assessment of soil bulk density. *Soil and Tillage Research*, *134*, 97 - 110. https://doi.org/https://doi.org/10.1016/j.still.2013.07.011

Suzuki, L. E. A. S., Reinert, D. J., Fenner, P. T., Secco, D., & Reichert, J. M. (2022). Prevention of additional compaction in eucalyptus and pasture land uses, considering soil moisture and bulk density. *Journal of South American Earth Sciences*, *120*, 104113. https://doi.org/https://doi.org/10.1016/j.jsames.2022.104113

van Verseveld, C. J. W., & Gebert, J. (2020). Effect of compaction and soil moisture on the effective permeability of sands for use in methane oxidation systems. *Waste Management*, *107*, 44-53. https://doi.org/https://doi.org/10.1016/j.wasman.2020.03.038

Wang, H., Wang, L., Huang, X., Gao, W., & Ren, T. (2021). An empirical model for estimating soil penetrometer resistance from relative bulk density, matric potential, and depth. *Soil and Tillage Research*, *208*, 104904. https://doi.org/https://doi.org/10.1016/j.still.2020.104904

Wang, Y., Kong, L.-w., Guo, A.-g., Tian, H.-n., & Qing, J.-s. (2009). Experimental research on gas permeability of shallow gassy sand in Hangzhou Metro Project. *Rock and Soil Mechanics, 30*(3), 815–819. http://ytlx.whrsm.ac.cn/CN/abstract/article_9599.shtml

Weeks, E. P., Earp, D. E., & Thompson, G. M. (1982). Use of atmospheric fluorocarbons F-11 and F-12 to determine the diffusion parameters of the unsaturated zone in the Southern High Plains of Texas. *Water Resources Research*. https://doi.org/10.1029/WR018i005p01365

Yu, C., Mawodza, T., Atkinson, B. S., Atkinson, J. A., Sturrock, C. J., Whalley, R., & Mooney, S. J. (2024). The effects of soil compaction on wheat seedling root growth are specific to soil texture and soil moisture status. *Rhizosphere*, *29*, 100838. https://doi.org/https://doi.org/10.1016/j.rhisph.2023.100838

Zhan, L.-t., Qiu, Q.-w., Xu, W.-j., & Chen, Y.-m. (2016). Field measurement of gas permeability of compacted loess used as an earthen final cover for a municipal solid waste landfill. *Journal of Zhejiang University-SCIENCE A*, *17*(7), 541-552. https://doi.org/10.1631/jzus.A1600245